Unification of the time and temperature dependence of dangling-bond-defect creation and removal in amorphous-silicon thin-film transistors

S. C. Deane, R. B. Wehrspohn,* and M. J. Powell
Philips Research Laboratories, Redhill, Surrey, RH1 5HA, United Kingdom
(Received 26 June 1998)

We present a thermalization-energy concept that unifies the time and temperature dependence of Si dangling-bond-defect creation and removal in amorphous-silicon thin-film transistors. There is a distribution of energy barriers for defect creation and removal, with the most probable energy barrier being 1.0 eV for defect creation and between 1.1 and 1.5 eV for defect removal, depending on how the defects were initially created. We suggest defect creation proceeds via Si-Si bond breaking, whereas defect removal proceeds by release of H from a SiHD complex. [S0163-1829(98)00243-4]

Thin-film transistors made from hydrogenated amorphous silicon exhibit metastable changes of the threshold voltage after prolonged applied bias to the gate electrode. Reasons for the threshold voltage shift have been discussed in the literature: Initially, charge trapping in the insulator was proposed as the instability mechanism.[1] However, measurements on ambipolar TFT's (Ref. 2) and the fact that the instability does not depend on the insulator (a-Si-N:H or SiO_2)[3] have unambiguously shown that the threshold voltage shift in the low-voltage stress region is due to metastable defect creation in the amorphous-silicon layer.

Metastable defect creation has been studied extensively for light-induced defects (Staebler-Wronski effect). However, there is still no consensus about the nature of the light-induced defects. The study of carrier-induced defect creation has mainly two advantages in comparison to light-induced defects: First, *one* type of carrier is present only (either electrons or holes depending on the type of the device). This facilitates the analysis of defect creation since no electron-hole recombination models have to be taken into account. Second, a *thermal barrier* for defect creation exists. For light-induced defect creation the recombination of an electron-hole pair provides the defect-breaking energy and the defect-creation process is essentially temperature independent providing no information about the energy barrier.

The threshold voltage shift during low-bias stress is generally fitted by a stretched exponential $\{1-\exp[-(t/t_0)^{\beta}]\}$, where experimentally t_0 exhibits an activated behavior $[t_0=\nu^{-1}\exp(E_a/kT)]$ and β is a slowly varying function of temperature. Several models have been proposed to account for this stretched exponential behavior,[4–6] which all result in the same differential equation:

$$\frac{d\Delta N_{\mathrm{DB}}}{dt} \propto -(\Delta N_{\mathrm{DB}})^{\alpha} t^{\beta-1} \tag{1}$$

where ΔN_{DB} is the number of metastable dangling bonds and $\alpha=1$ in order to obtain a stretched exponential.

The proposed models can be summarized into essentially two groups depending on the rate-limiting step during defect creation. This step is either the charge-induced breaking of the silicon-silicon bond (exponential barrier-distribution model[6]) or the stabilization of a broken bond by hydrogen (dispersive hydrogen-diffusion model[4,5]). Note that both of these models make the assumption that T/β is a constant, equal to the Urbach energy. It has been recently shown that this assumption could only be maintained over a quite small temperature range and that β becomes temperature independent for $T>360$ K.[7] Moreover, in the linear range, β seems not to be proportional to T but exhibits a linear behavior $(\beta=T/T_0-\beta_0)$ which could not be explained by any of the proposed models.

The bias stress experiments have been carried out on n-type, silicon-nitride gate insulator a-Si:H TFT's deposited at 300 °C on crystalline silicon wafers. The preparation conditions were reported elsewhere.[8] All TFT's have been annealed at 500 K before the stress experiment in order to have identical initial conditions.

In Fig. 1, typical bias-stress curves for $V_{\mathrm{bias}}=30$ V, $t=10^5$ s, and $T=303$, 343, and 383 K are plotted as $-\ln\{\Delta V_t(t)/[V(\infty)-V(0)]+1\}$ over t on a double-logarithmic scale, where $V(\infty)$ is the applied gate bias and $V(0)$ is the initial threshold voltage. In this format, a stretched exponential dependence gives a straight line. The 303 K bias-stress curve exhibits a stretched exponential behavior over the range measured. However, for $T=343$ K a stretched exponential can be obtained only for $t<10^4$ s, and for $T=383$ K there is no stretched exponential behavior. From the linear fits, β and t_0 can be determined. The parameter t_0 exhibits an activated behavior with an activation energy of about 0.99 eV and a corresponding attempt-to-escape frequency of about 10^{10} Hz. The parameter β exhibits a linear relationship with T up to 363 K and then saturates at a value of 0.52. In the linear regime, $T_0=450$ K and an offset of about $\beta_0=-0.28$ has been obtained. These results are quite similar to those obtained in Ref. 7. Note that there are several possible ways to determine β from the bias-stress data. One may either directly fit the data by a stretched exponential least-square fit or make a power-law fit for small time scales as was done earlier.[9] These two methods, and that described above, have been applied for the $T=303$, 343, and 373 K experiments. Whereas for the 303 K, all methods give the same parameters, for the $T=343$ K and the $T=383$ K experiments, a strong variation mainly in the β parameter is obtained. Therefore, the β parameter is not a good way to describe the degree of instability of a TFT.

 ©1998 The American Physical Society

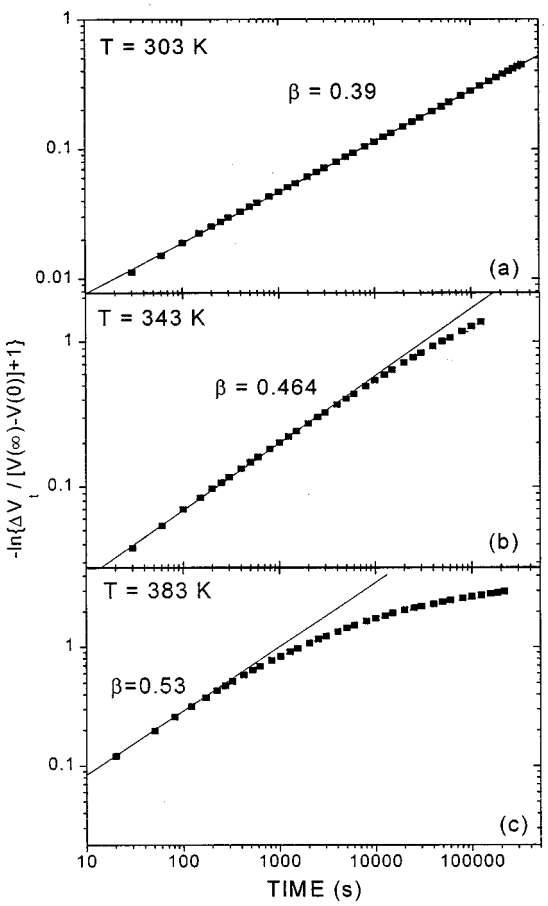

FIG. 1. Threshold voltage shifts during bias stress ($V_{\text{bias}}=30$ V) for $T=303$ (a), 343 (b) and 383 K (c) on a $\log_{10}[-\ln\{\Delta V_t/[V(\infty)-V(0)]+1\}]$ vs $\log_{10}(t)$ plot. The data have been fitted to a stretched exponential $\{1-\exp[-(t/t_0)^{\beta}]\}$, which reads a straight line in this format.

A unique description of the instability with stronger physical meaning is given by the thermalization-energy concept. It has been shown by various techniques, e.g., field-effect analysis, that metastable defects (here in units of cm^{-2}) are created during bias stress according to the relationship[3]

$$\Delta N_{\text{DB}} \approx \frac{\varepsilon_0 \varepsilon_{\text{ins}}}{q d_{\text{ins}}} \Delta V_t, \tag{2}$$

where ε_{ins} and d_{ins} are the dielectric constant and the thickness of the insulator, respectively.

In analogy to the equilibrium-defect reaction,[10] these metastable defects created during bias stress could only be stable if hydrogen motion is involved. Thus, quite general overall creation reactions are

$$\text{Si}-\text{Si}+\text{SiH} \xrightarrow{e^-} \text{SiHD}+\text{D} \tag{3a}$$

or

$$\text{Si}-\text{Si}+\text{SiHHSi} \xrightarrow{e^-} 2\text{SiHD}, \tag{3b}$$

where the defects D or SiHD are either charged or neutral.

It has been shown that defect creation during bias-stress exhibits an activated behavior (contrary to defect creation by light soaking). This implies that a thermal barrier for defect creation exists during bias stress. In thermal equilibrium (~500 K), this barrier is not important and the detailed balance of defect creation and removal is governed by the formation energy of the defects. It has been shown recently[10] that defects created at equilibrium can be described with a hydrogen density-of-states diagram (Fig. 2). In this picture, the maximum of the equilibrium-defect distribution is at the energetically lowest level, i.e., mainly Si-Si bonds with high strain or distortion have converted to dangling bonds. Since this is an equilibrium process, the intermediate steps to arrive at this distribution, for example, trapping of hydrogen by breaking a Si-Si bond and hydrogen release involving the rebonding of the two silicon atoms, are not relevant for the solution of the equilibrium model. However, in nonequilibrium, the specific intermediate step depends mainly on the energy barrier and not on the formation energy.

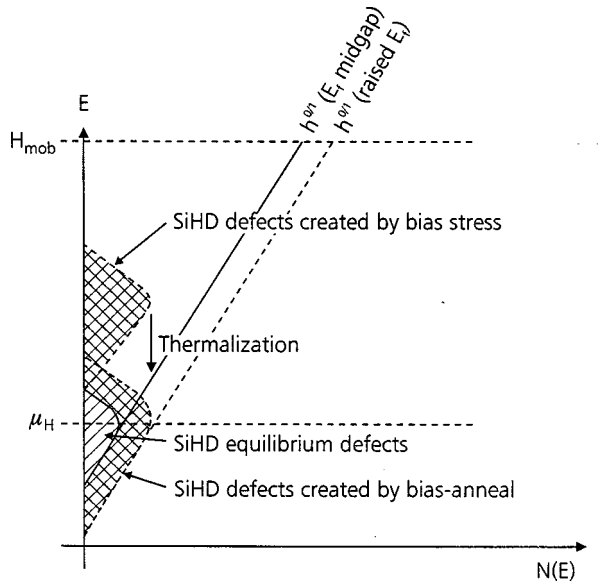

FIG. 2. Model of the hydrogen density of states (H-DOS) after Ref. 10. Here, only the transition Si-Si⇔SiHD is represented ($h^{0/1}$ transition). In equilibrium without applied bias, defects are created around the hydrogen chemical potential in the lower part of the $h^{0/1}$ tail. If the Fermi level changes (doping, bias stress, light soaking), the absolute H-DOS tail-state density shifts towards higher values. During bias stress, defects are created mainly in the upper part of the H-DOS and then thermalize down the $h^{0/1}$ tail depending on the temperature at which they have been created.

Assuming a monomolecular-creation mechanism, the creation kinetics for a unique activation energy would be a simple exponential in contradiction with the experimental results (Fig. 1). Following Stutzmann, Jackson, and Tsai,[11] we therefore assume a distribution of energy barriers $D(E_a)$, which could account for the observed kinetic behavior. This distribution may be either due to a distribution of ground states (weak bonds), a distribution of barrier heights, or both. To a first-order approximation, after a time t at a temperature kT all possible defect-creation sites with $E_a \leqslant kT\ \ln(\nu t)$ will then have converted into defects. The thermalization energy is therefore defined by

$$E = kT\ \ln(\nu t), \tag{4}$$

where ν is the attempt-to-escape frequency.

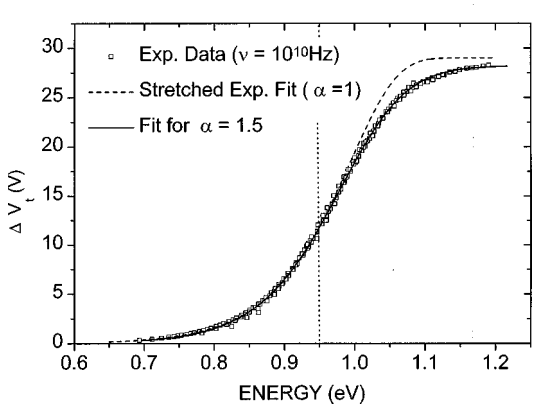

FIG. 3. Threshold voltage shifts ($V_{\text{bias}}=30$ V) for different times ($1<t<10^5$ s) and temperatures (303 K$<T<$403 K) unified in terms of the thermalization energy $E=kT\ \ln(\nu t)$. The solutions of Eq. (1) for $\alpha=1$ (stretched exponential, plotted as dashed line) and for $\alpha=1.5$ (solid line) as a function of the thermalization energy are shown for comparison (see text).

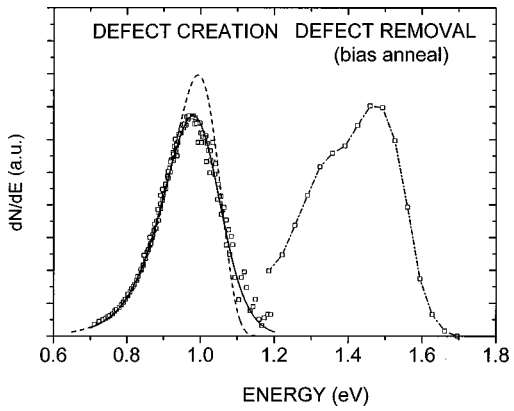

FIG. 4. Probability distribution of activation energies for defect creation and defect removal. The data have been obtained by taking the derivative of the threshold voltage shifts for defect creation (Fig. 3) and defect relaxation. In the latter case, threshold voltage shifts have been determined by annealing the device without applied bias to different temperatures after bias stress ($V_{\text{bias}}=30$ V) at 500 K for $1h$. The derivative of the solution of Eq. (1) for $\alpha=1$ (stretched exponential, plotted as dashed line) and for $\alpha=1.5$ (solid line) as a function of the thermalization energy are shown for comparison (see text).

Now, we apply the concept of thermalization energy to the bias-stress data [Figs. 1(a)–1(c)]. Figure 3 shows the threshold voltage shift as function of the thermalization energy for a series of bias-stress experiments carried out at temperatures between 303 and 403 K. A unique curve is obtained with only *one* fit parameter, the attempt-to-escape frequency, which we find to be about 10^{10} Hz. An even clearer physical picture is given by the derivative of the bias-stress curve, i.e., the number of created defects per thermalization energy interval (Fig. 4). The maximum of this distribution represents the most likely defect-creation energy barrier and the width of the curve reflects the probability distribution of energy barriers, i.e., the density of possible sites with a barrier E_a multiplied by the probability of occupation of such site. These parameters give a unique indication of the device stability in that they allow accurate scaling to all times and temperatures. In Fig. 4, the maximum of the distribution is at about 0.975 eV and its full width at half maximum is about 0.18 eV.

In both the hydrogen diffusion model[4] and the exponential barrier distribution model,[6] a stretched exponential as a function of the thermalization energy will then read $\exp\{-\exp[(E-E_a)/kT_0]\}$ assuming that β is proportional to the temperature and t_0 is activated with an activation energy of E_a. Plotting a stretched exponential as a function of the thermalization energy is shown in Fig. 3. The stretched exponential still describes the data reasonably well for $E<0.95$ eV but for $E>0.95$ eV, the experimental curve exhibits a clear deviation. A possible explanation may lie in the bandtail-carrier dependence. To obtain a stretched exponential, the defect-creation rate has to be proportional to the number of excess bandtail carriers ΔN_{BT}, i.e., $\alpha=1$ in Eq. (1). However, we find experimentally by varying the gate bias that the defect-creation rate is proportional to $(\Delta N_{\text{BT}})^{\alpha}$ with α between 1.5 and 1.7 (in agreement with Ref. 12). Solving Eq. (1) for $\alpha=1.5$, we obtain $\Delta V_t \propto [(t/t_0)^{\beta}+1]^{-2}$ and a much better fit for thermalization energies $E>0.95$ eV is obtained (Fig. 3). For $E<0.95$ eV, a stretched exponential and the solution for $\alpha=1.5$ are nearly identical since the number of bandtail carriers remains approximately constant ($N_{\text{DB}} \ll N_{\text{BT}}$) in this region of the curve. Calculating β by the new formula as a function of the temperature, a linear relationship is obtained with $T_0=720$ K and $\beta_0=0$. The value of $\alpha>1$ could result either from a carrier-dependent hydrogen-diffusion constant[6] or from an additional weakening of an occupied conduction-bandtail state by multielectron interaction. However, the elegance of the thermalization energy concept is that it is independent of these specific microscopic mechanisms.

The same concept of thermalization energy can also be applied to defect removal as reported previously.[13] It has been shown previously that samples where defects have been created by bias stress show an energy-barrier distribution for defect removal with a maximum around 1.1–1.4 eV depending on the time and temperature at which the defects were created. For samples where defects are created by bias annealing (bias applied during equilibration), the maximum of the energy distribution of defect removal shifts to about 1.5 eV as shown in Fig. 4. *All* states, whether created by bias stress or bias anneal are subsequently removed with an attempt-to-escape frequency of about 10^{13} Hz.

These distributions can be interpreted by different thermalization depths. During defect creation, a silicon-silicon bond may be broken even if the formation energy is not at a minimum. The SiHD complex then tries to minimize its energy by breaking another silicon weak bond with a lower formation energy:

$$\text{Si}-\text{Si}_{\text{weak}}+\text{SiHD}\rightarrow\text{SiHD}+\text{Si}-\text{Si}_{\text{strong}}. \tag{5}$$

This process can be understood as a thermalization of the SiHD defect in the $h^{0/1}$ hydrogen density of states (Fig. 2), in analogy with an electron that thermalizes down the band tails.[10]

Comparing defect creation and removal shows that the defect-creation process ($E_a=0.975$ with $\nu_0=10^{10}$ Hz) and the defect-removal process ($E_a=1.1$–1.5 eV with ν_0

$=10^{13}$ Hz) have different barrier heights and different prefactors. Due to the thermalization of the SiHD defect in the hydrogen density of state (DOS), the defect creation path is not the same as the defect-removal reaction. A plausible defect-creation reaction is the breaking of a weak Si-Si bond, its saturation by back-bonded hydrogen, and then *local* switching of the SiHD defect in order to minimize its energy in the H-DOS (Fig. 2). On the other hand, defect removal is more likely due to the release of hydrogen out of a SiHD complex and then involves *long-range* interstitial hydrogen motion. This picture is supported by the fact that the attempt-to-escape prefactors for defect removal and defect creation are significantly different. Whereas 10^{13} Hz is the typical phonon frequency of a Si-H bond, the lower frequency of 10^{10} Hz for defect creation might result from a stronger lattice coupling as expected for Si-Si bonds.

Finally, our results show strong similarities to those obtained by light soaking indicating similar microscopic processes. For defect removal, Stutzmann, Jackson, and Tsai[11] have found an energy-barrier distribution that peaks at 1.1 eV for defects created at room temperature and about 1.2 for post-annealed samples ($T_a = 110\ ^\circ$C). Even if these different maxima have been initially interpreted by a distribution of defect energies,[11] these values are in good agreement with our defect removal data,[13] and could also be explained in the concept of thermalization in the hydrogen DOS (Fig. 2).

In conclusion, we have shown that the concept of thermalization energy gives a description for defect creation and removal over a wide range of times and temperatures independently of the specific microscopic mechanisms. The width and the peak position of the distribution of activation energies give a good indication for the stability of the device with a strong physical meaning. The most probable energy barrier during defect creation is around 1 eV with a corresponding attempt-to-escape frequency $\nu = 10^{10}$ Hz, whereas for defect removal $\nu = 10^{13}$ Hz and the most probable energy barrier lies between 1.1 and 1.5 eV depending on the temperature at which the defects have been created. This indicates that the microscopic reaction paths involved in defect creation and defect removal are different with different rate-limiting steps.

*Electronic address: wehrspoh@prl.research.philips.com

[1] M. J. Powell, Appl. Phys. Lett. **43**, 597 (1983).
[2] C. van Berkel and M. J. Powell, Appl. Phys. Lett. **51**, 1094 (1987).
[3] M. J. Powell *et al.*, Phys. Rev. B **45**, 4160 (1992).
[4] J. Kakalios, R. A. Street, and W. B. Jackson, Phys. Rev. Lett. **59**, 1037 (1987).
[5] W. B. Jackson, Phys. Rev. B **41**, 1059 (1990).
[6] R. S. Crandall, Phys. Rev. B **43**, 4057 (1990).
[7] F. R. Libsch and J. Kanicki, Appl. Phys. Lett. **62**, 1286 (1993).
[8] S. C. Deane *et al.*, J. Appl. Phys. **73**, 2895 (1992).
[9] M. J. Powell, C. van Berkel, and J. R. Hughes, Appl. Phys. Lett. **54**, 1323 (1989).
[10] M. J. Powell and S. C. Deane, Phys. Rev. B **53**, 10 121 (1996).
[11] M. Stutzmann, W. B. Jackson, and C. C. Tsai, Phys. Rev. B **32**, 23 (1985).
[12] Y. Kaneko, A. Sasano, and T. Tsukada, J. Appl. Phys. **69**, 7301 (1991).
[13] P. N. Morgan *et al.*, in *Amorphous Silicon Technology—1994*, edited by E. A. Schiff *et al.*, MRS Symposium Proceedings No. 336 (Materials Research Society, Pittsburgh, 1994), p. 811.